42nd Conference on
Our World in Concrete & Structures
23-25 August 2017, Singapore

SHEAR PERFORMANCE OF PRECAST PRE-STRESSED CONCRETE BEAMS USING UNBONDED TENDONS

Kazushi SHIMAZAKI*, Yuki SHIRAI† and Naoki YAGINUMA‡

*Kanagawa University
Rokkakubashi 3-27-1, Kanagawa-ku, YOKOHAMA, JAPAN
Email: shimazaki@kanagawa-u.ac.jp
Webpage: http://shimazaki.arch.kanagawa-u.ac.jp/

Keywords: Pre-stressed Concrete, Unbonded, Shear Performance

Abstract. *Shear-bending tests for precast pre-stressed concrete beams using unbonded tendons were carried out. The test results for the small shear span to depth ratio specimens showed shear failure with a diagonal crack across the beam and decreasing shear force immediately. The truss-arch mechanics method using effective concrete strength accurately evaluates the shear strength. This method concurs with the shear strength decreasing while deformation of the beam increases. For the other specimens, bending failure occurred and shear force slowly decreased. The ACI stress block method accurately evaluates the flexural strength. Tie bars for shear reinforcement are effective at maintaining shear strength after failure, even in the event of a shear failure.*

1 INTRODUCTION

Precast pre-stressed concrete beams using unbonded tendons suffer intensive earthquake-induced small residual cracks and damage only at their joints. By repairing these joints, this structure is quickly returned to use as a facility after the earthquake, and is expected to afford long-term service use. In contrast to bending performance, no method has been established to evaluate the shear performance of this type of beam.

This study aims to evaluate the shear performance of the precast pre-stressed concrete beam using unbonded tendons through tests and analyses. Initially, shear-bending tests are carried out for nine specimens. These specimens consist of a beam part and two stubs which interpose the beam. Two tendons connect the beam and the stubs. The stubs are controlled to be parallel and an anti-symmetric bending moment is applied to the specimens. The test parameters are shear span to depth ratio (1.0 and 1.5), shear reinforcement ratio (0.28% ~ 1.26%) and shear reinforcement arrangement (presence of tie bar). Next, a finite element method analysis is carried out. Three-dimensional models that fit the test specimens are created. This analytical study examines the internal stresses of the concrete.

†Assistant Prof., Dept. of Architecture and Building Engineering, Kanagawa University, D.Eng.
‡Kanagawa University (former graduate student)

2 OUTLINE OF EXPERIMENTS

2.1 Test specimens

The test specimen list is shown in Table 1. The specimen shapes and the typical bar arrangements are shown in Figure 1. Parameters are shear span ratio (1.0 and 1.5), shear reinforcement ratio (0.28% ~ 1.26%), shear reinforcement interval, and the presence of tie bars. The beam section is 250 mm by 450 mm, and the lengths are 900 mm or 1,350 mm. The initial pre-stress forces were 1,320 [kN] (σ/Fc=0.26, σ: compression stress, Fc: Design concrete strength = 45 N/mm²).

No.		PC08	PC09	PC10	PC11	PC12	PC13	PC14	PC15	PC16
Length(mm)		900			1350			900		
Section(b×D)		250×450								
Concrete	F_c (N/mm^2)	45								
	σ_B (N/mm^2)	52.6			69.6			59.6		
Shear Span Ratio		1.0			1.5			1.0		
PC bar ϕ (mm)		#C 2-φ32								
Shear Reinforcements		D6-S@90	D6-W@90	D10-W@90	D6-S@90	D6-W@90	D6-W@70	D6-W@70	D10-S@70	D10-S@90(45)
Ratio [%]		0.28	0.56	0.127	0.28	0.56	0.73	0.73	0.82	0.64
Axial Reinforcements		4-D16	8-D13		4-D16	8-D13		8-D13	4-D16	
Design strength	Q_c (kN)	416								
	Q_u (kN)	494	548	686	328	390	427	584	601	601
	M_u (kNm)	225								
	Q_{Mu} (kN)	501			334			501		

Table 1: Test Specimens.

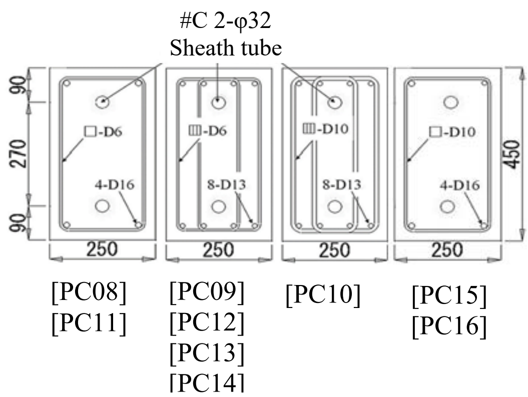

(a) Section

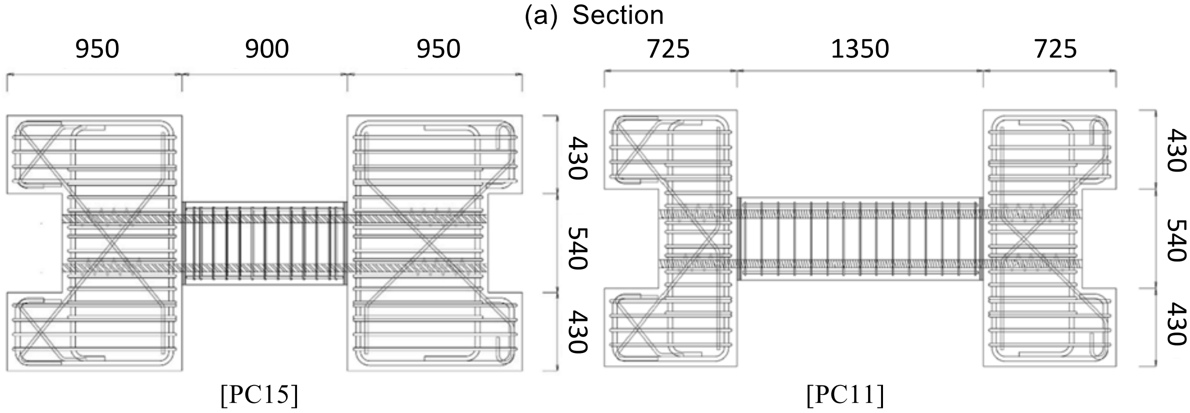

(b) Overall view of typical specimen

Figure 1: Section and overview of specimens

PC08 is the basic form. PC09, 10 and 14 have a larger shear reinforcement ratio than PC08. The presence of tie bars in PC09 and 10 differs, PC10 has a different bar section with the same reinforcement spacing. PC15 has the same shear reinforcement ratio as PC14 while eliminating the tie bars, and the presence or absence of tie bars makes a difference. PC16 has the same number of shear reinforcements as PC15, but the reinforcements were concentrated at the end of the member, to assess restraining of the concrete at the end of the member. PC11, 12, and 13 have a shear span ratio of 1.5 and are to investigate the difference with the specimen with a shear span ratio of 1.0. PC11 and 12 differ in the presence or absence of tie bars, with PC12 and 13 having different reinforcement spacing.

On the design of specimens, the shear cracking strength (Q_c) was calculated using the maximum principal stress, as per Equation (1)[1]. The ultimate shear strength (Q_u) was calculated using the arch-truss theory, as per Equation (2)[2]. The ultimate flexural strength (M_u) was calculated using the ACI stress block method with the compression stress as the pre-stressing force at the time of introduction. The calculated values are shown in Table 1.

$$Q_c = \sqrt{{\sigma_t}^2 + \sigma_t \cdot \sigma_0} \cdot b \cdot D/1.5 \tag{1}$$

$$Q_u = bj_o p_w {}_w f_y + \frac{bD}{2}\left(\nu\sigma_B - 2p_w {}_w f_y\right) tan\theta \tag{2}$$

where, σ_t: Tensile strength of concrete = $0.33\sqrt{\sigma_B}$ [N/mm^2], σ_B: Compressive Strength of concrete [N/mm^2], σ_0: Axial stress [N/mm^2], b: Width [mm], D: Depth [mm], j_o: Distance from center of compressed rebar to center of tensile rebar [mm], p_w: Shear reinforcement ratio, ${}_w f_y$: Yield strength of shear reinforcement [N/mm^2], $\nu = \alpha L_r\left(1 + \frac{\sigma_g'}{F_c}\right), \alpha = \sqrt{60/\sigma_B}, L_r = \frac{M}{2QD}, \sigma_g' = P/(bD)$ [N/mm^2], $tan\theta = \sqrt{\left(\frac{2M}{QD}\right)^2 + 1} - \frac{2M}{QD}$

2.2 Measurement plan

Figure 2 shows the displacement measurement points. Overall longitudinal direction deformation of the specimen was measured with a displacement-measuring device installed between the upper and lower stubs. As shown in the figure, the displacement measuring devices were arranged continuously in the axial direction on the side surface of the beam, and the section deformations were measured to separate the bending deformation and the shear deformation. Strain gauges were attached to the PC bars, axial reinforcement bars, and shear reinforcement bars. The crack width was measured using a crack scale at the peak loading cycles and unloaded point.

2.3 Test setup and load control

The test setup is shown in Figure 3. The main actuator, which was mounted at a position corresponding to the center height of the specimen from the reaction force wall, applied the horizontal force. The upper stub was controlled to be parallel to the lower stub by using two sub-actuators. Positive and negative static repetitive loading was applied twice in the order R=1/800, 1/400, 1/200, 1/133, 1/100, 1/67, 1/50, and was applied once at 1/33 and 1/25.

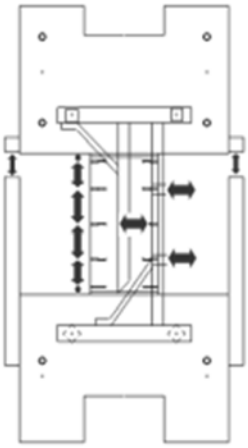

Figure 2: Displacement measurement

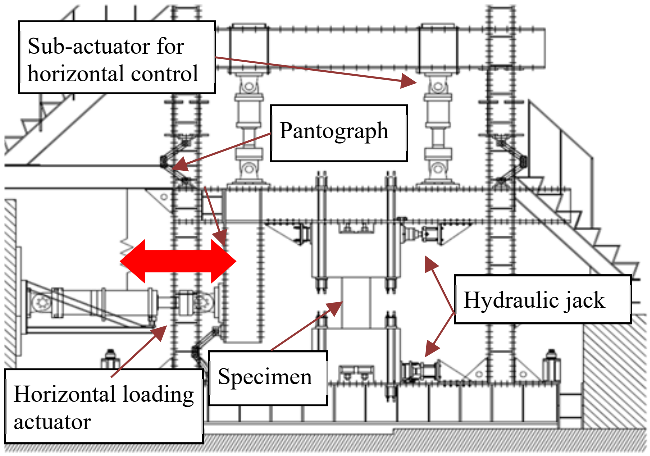

Figure 3: Test setup

3 TEST RESULTS

The shear force-deformation relationship is shown in Figure 4, and the final damage status is shown in Photo 1.

In PC08, a shear crack was observed at R=-1/133 (first time), a shear fracture occurred at R=-1/133 (second time), and the shear force suddenly decreased. In PC09, a shear crack was observed at R=1/200 (first time), shear fracture occurred at R=1/67 (first time), and the strength sharply decreased. In both PC08 and PC09, crushing of concrete at the end was observed at R=1/200. In the PC10, shear cracks occurred at R=1/133 (first time), signs of crushing were seen at the edge at R=1/100. As the step progressed, crushing at the end progressed, and the shear crack width increased. At R=-1/33, crushing of the end portion progressed, the formation of the compression strut collapsed, and as a result, the strength declined at R=±1/25.

In PC11-13, at R=1/100, only the joint portion is open, and even if damage at the end progresses, shear cracks will not eventually enter the central portion. In PC11 with the least shear reinforcement, the strength was retained until R=1/50. It was R=1/33 for PC12 and was R=1/25 for PC13, which had the most shear reinforcement. In these specimens, almost no residual deformation occurred even after substantial deformation of R=1/25.

In PC14, the signs of edge crushing of the concrete occurred at R=1/200 (first time), shear cracking occurred at R=-1/200 (second time), and it was destroyed at R=1/33. In PC15, edge crushing occurred at R=1/133 (second time), shear cracking occurred at R=-1/133 (second time), and bending cracking occurred at R=1/50 (first time). It was destroyed at R=1/33. In PC16, edge crushing occurred at R=1/133 (first time), shear cracking occurred at R=1/100 (second time), and it was destroyed at R=1/50.

Damage progress statuses for all specimens and the maximum strength are summarized in Table 2.

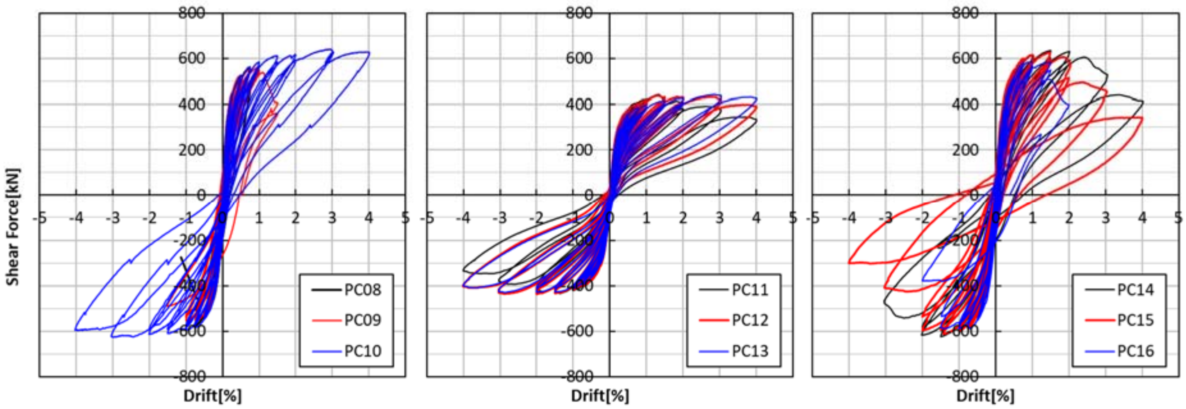

Figure 4: Load-deformation relationship

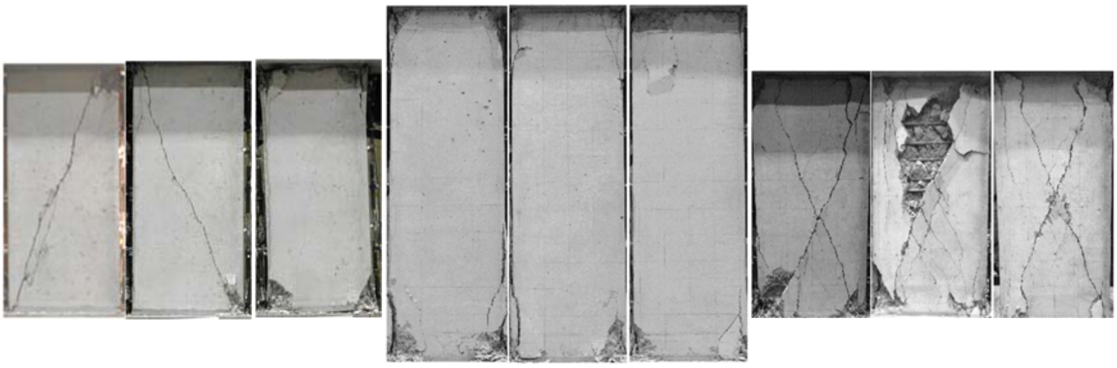

PC08 PC09 PC10 PC11 PC12 PC13 PC14 PC15 PC16

Photo 1: Final damage

□:Bending crack ◇:Shear crack ■:Edge crushing ☆:Max. strength ×:Shear fracture

Drift Angle(%)	R=0.25	R=0.5	R=0.75	R=1.0	R=1.5	R=2.0	R=3.0	Max. strength (kN)
PC08		■	◇☆×					574
PC09		■◇		☆	×			564
PC10				■	◇		☆	643
PC11	△	□■		◇	☆			441
PC12	△	□	■	◇	☆			437
PC13	△□	■					☆	442
PC14		□			☆		×	635
PC15			■		☆	×		626
PC16			■	◇	☆	×		589

Table 2: Damage Progress

4 ULTIMATE STRENGTH

4.1 Shear strength

Figure 5 shows the shear force-deformation relationship between the 1.0 shear span ratio specimens. These specimens except PC08 are considered to have experienced shear fractures after bending yield (compression side). Although the maximum strength hardly changes, the amount of deformation that can still retain the strength increases as the shear reinforcement ratio increases. Between PC14 and 15, the shear reinforcement ratio is slightly larger in PC15, but the reinforcing pitch is the same. PC15 has a large reinforcing bar diameter without tie bars. There was no difference in the maximum strength, but there was a difference in the strength at R=4.0 [%]. It seems the internal compression strut against the arch mechanism was retained by the constraining effect of the tie bars. It can be said that not only the shear reinforcement ratio, but also the presence or absence of a tie bar, are factors in the strength retention ability after the maximum strength.

In the reference,[1] Equation 3 gives the decrease in shear strength (Q_u) due to the increased damage with the increasing deformation.

$$Q_u = \mu p_{we}\sigma_{wy}b_e j_e + \left(\nu\sigma_B - \frac{5p_{we}\sigma_{wy}}{\lambda}\right)\frac{bD}{2}\tan\theta \quad (3)$$

where, μ: coefficient of truss mechanism angle = 2-20 R_p, R_p: Rotation angle of hinge region (Member rotation in this paper), p_{we}: Shear reinforcement ratio, σ_{wy}: Yield strength of shear reinforcement [N/mm^2], b_e: Effective width, j_e: Effective depth, $\nu = (1-20R_p)\nu_0$, ν_0 : Effective factor (=1.0 in this paper), σ_B : Compressive Strength of concrete [N/mm^2], λ: Effective coefficient of truss mechanism, b: Width [mm], D: Depth [mm], $tan\theta = \frac{\sqrt{L^2+D^2}-L}{D}$ for $\mathrm{L/D} < 1.5$, L: Clear member span [mm]

In Figure 5, the decreases in shear strength with increasing deformation calculated by Equation (3) for the typical specimens are drawn by dash-dotted lines. The decrease tendency of the shear strength with increasing deformation and the degree of strength reduction depending on the shear reinforcement ratio can be simulated.

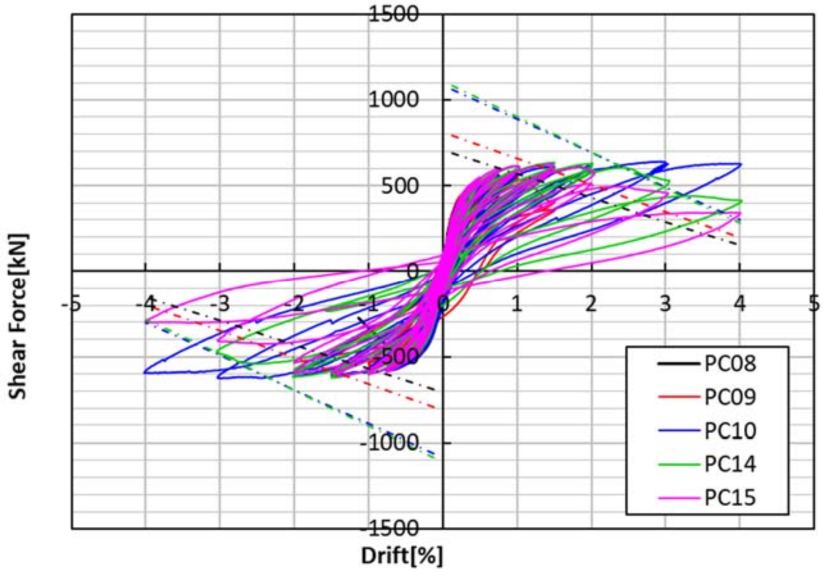

Figure 5: Load-deformation relationship of 1.0 shear span ratio specimens

4.2 Flexural strength

The PC11-13 specimens, whose shear span ratio is 1.5, and PC10 with its heavy shear reinforcement from a shear span ratio of 1.0, did not experience shear failure even at R=4.0 [%]. The ultimate flexural strength was calculated using the ACI stress block method. As the deformation progresses, additional stress is generated on the PC bars because the beams extend geometrically. Figure 6(a) shows the relationship between deformation and the tension stress of the PC bar for PC11. Because of the asymmetric bending, the fluctuations in the two tension bars are almost the same. Tension stress increases linearly with deformation. However, it seems there is an upper limit at about R=2% deformation. The deformation indicating this upper limit is at about R=3% in PC13. It seems that the confined effect due to transverse reinforcement appears. Also, the tension decreases due to repetitive damage to the end concrete. Figure 6 (b) shows the shear force – Axial force relationship of each specimen. The maximum axial force is 1,600 kN for PC10 and 11 and 1,750 kN for PC12 and 13. Calculating the shear force at the ultimate flexural strength with these axial forces, these are 545 kN (this becomes 600kN when β_1 keeps value of 0.85 considering confined effect of transverse reinforcements) for PC10, 404 kN for PC11, and 430 kN for PC 12 and 13 as shown in Figure 7. The calculated values are slightly small, but they correspond roughly to the experimental values shown in Table 2.

The shear cracking strength according to Equation 1), using the actual strength was 474 kN, which was larger than the maximum experimental strength in the test specimens with a shear span ratio of 1.5, as shown in Figure 7(b).

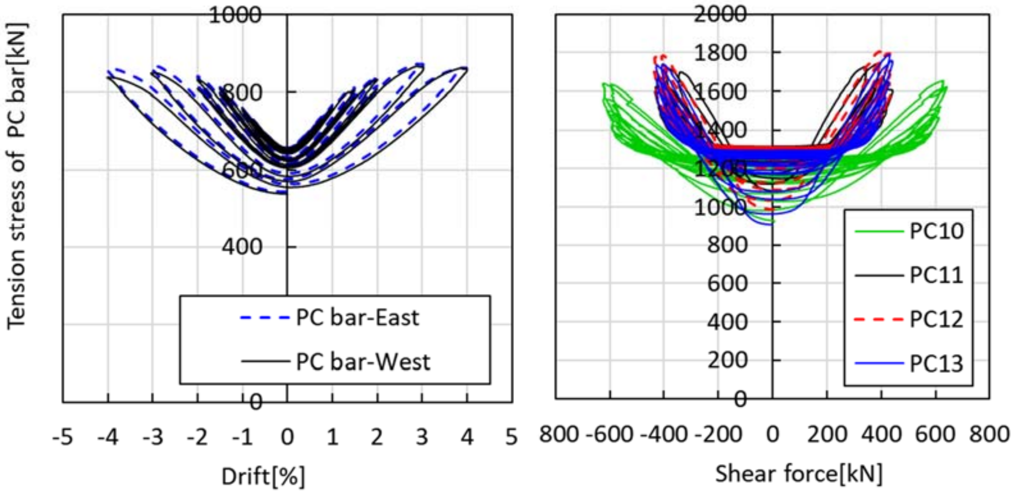

(a) PC Tension stress of PC bars (b) Shear force – PC bar stress relationship

Figure 6: Variation in PC bar tension stress

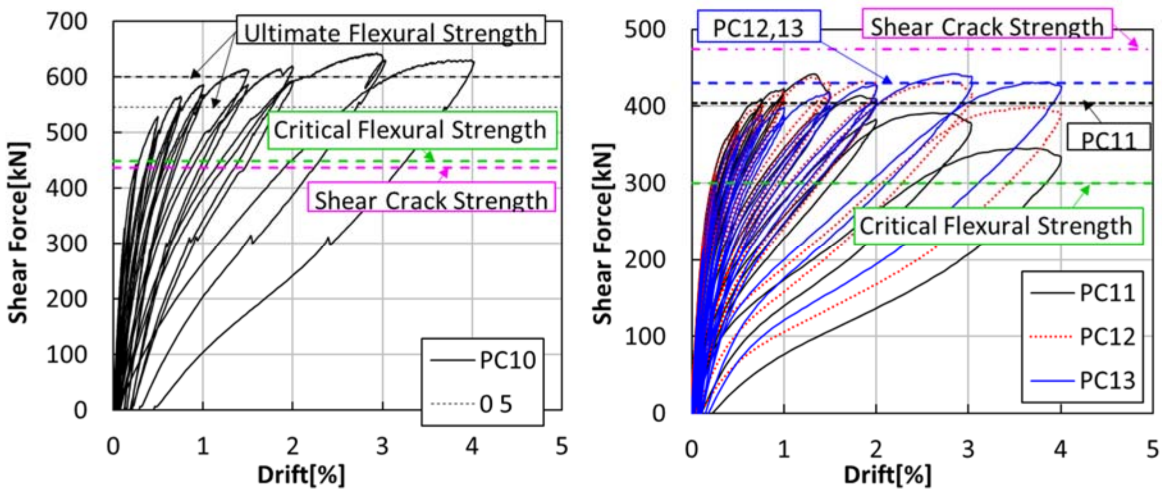

(a) 1.5 shear span ratio specimens (b) 1.0 shear span ratio specimens

Figure 7: Comparison of the ultimate flexural strength

5 SERVICEABILITY LIMIT STATE STRENGTH

5.1 Shear strength

The shear damage limit critical strength is determined with consideration for the residual crack width after shear cracking, but the shear crack proof stress of the PC member is large because the pre-stressed force acts as an axial force. Therefore, shear crack resistance strength can be considered as the shear damage limit critical strength.

5.2 Flexural strength

Based on Reference 2), the damage critical compressive stress of concrete was set as 0.9 times the cylinder strength of concrete, and the critical flexural strength at the serviceability limit state was calculated assuming a triangular stress distribution of the concrete. Ignoring the fluctuation of the caulking force of the PC steel bar by using the actual strength, the distance from the compression end to the neutral axis is 168.6 mm. The shear force at the critical flexural strength is 300 kN for all specimens with a 1.5 shear span ratio, and is 448 kN for PC10 as shown in figure 7. Up to this shear force, no damage was observed and little residual deformation occurred. Therefore, this flexural strength can be considered as the flexural damage limit critical strength.

6 EFFECTS OF SHEAR REINFORCEMENTS

Figure 8 (a) shows the strain distribution of the shear reinforcements at R=1% and 4%, for specimens with a shear span ratio of 1.0. PC10 did not experience shear failure. The shear reinforcement bars did not yield, and the strain values are smaller at the end than in the middle. As PC14 and 15 were destroyed by shear, the shear reinforcements yielded in the middle. Even so, the shear reinforcements in the end portion still did not yield. Figure 8 (b) compares the strains on outside bars and tie bars in terms of shear reinforcements. There is no significant difference between outside bars and tie bars for either PC10, which did not experience shear failure, and PC14 – which did. Figure 8 (c) shows the strain distribution of the shear reinforcements at R=1% and 4%, for a shear span ratio of 1.5. Since no shear cracks occurred in the middle, the strain values are small. The values become larger at the ends. This value increases as the shear reinforcement ratio decreases. This is because the shear reinforcements are effective for restraining the concrete as lateral reinforcements at the end portion and corresponds to the capacity holding ability in the shear force-deformation relation of Figure 7(b).

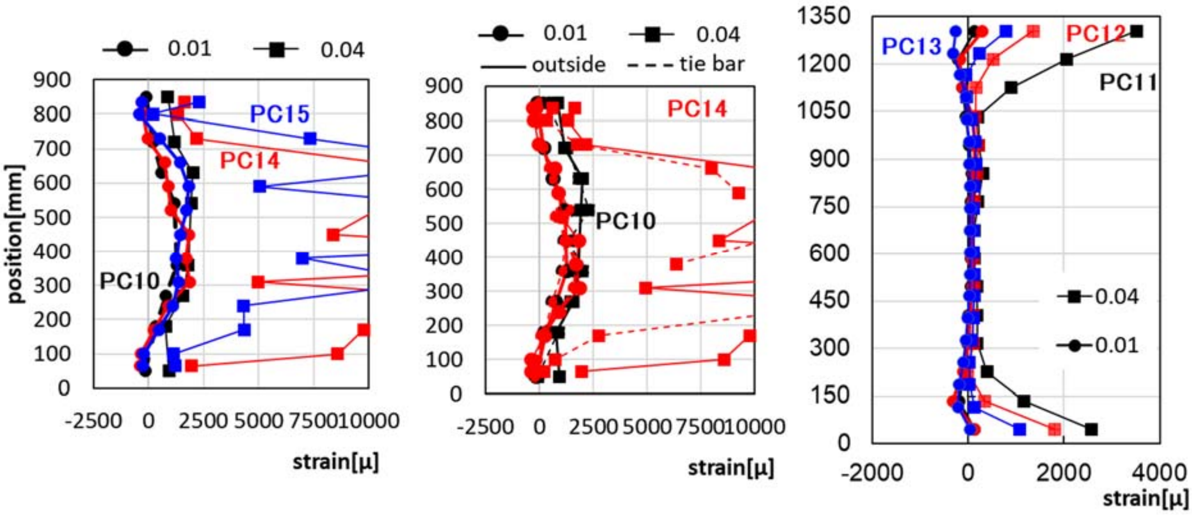

(a) Shear span=1.0 (b) Comparison with tie bar (c) Shear span=1.5

Figure 8: Strain distribution of shear reinforcements

In order to consider the influence of the tie bar, FEM analysis was carried out using the general-purpose finite element method program (FINAL ver. 11)[3] for PC14 and PC15, which have the same shear span ratio of 1.0 and similar shear reinforcement ratio. The differences between them are in the presence or absence of tie bars; specifically PC14 has a tie bar. Concrete, joint mortar, steel plates and loading jigs were modeled as an eight-node element. The reinforcing bar and PC bar were modeled as a two-nodal-point truss element. The material strength used the value obtained in the material test. As hysteresis characteristics of concrete, the characteristics on the tensile side were linear before cracking, and after cracking, tension stiffening was taken into account using the Izumo model.[4] For the compression side, the modified Ahmad model was used up to the maximum strength and strain softening was considered after the maximum strength.[5] For the strain softening characteristics after cracking, Naganuma's proposed formula was used.[5] The stress-strain relationship between reinforcing bars and PC steel bars was defined by a bilinear model. The pre-stress force was applied to the PC-bar-fixing-steel-plate as a compressive force, and the horizontal force was monotonically loaded to the tip of the load-applying jig located by aiming at the middle of the specimen as per the experiment. Figure 9(a) shows the analysis model.

A comparison between the analysis results and the experiment into the shear force-deformation relationship is shown in Figure 9(b), with PC14 used as an example. The analytical results enable the rigidity and strength to be successfully followed. Figure 9(c) shows the minimum principal stress diagram of a cross-section at the central height of the specimen when the shear force was 588 kN. In the case of PC14, which has a tie bar, there is a large compression stress in the core, and the compression strut of the concrete in the arch mechanism is held, but in PC15 which lacks a tie bar, the compression strut for the core part cannot be seen.

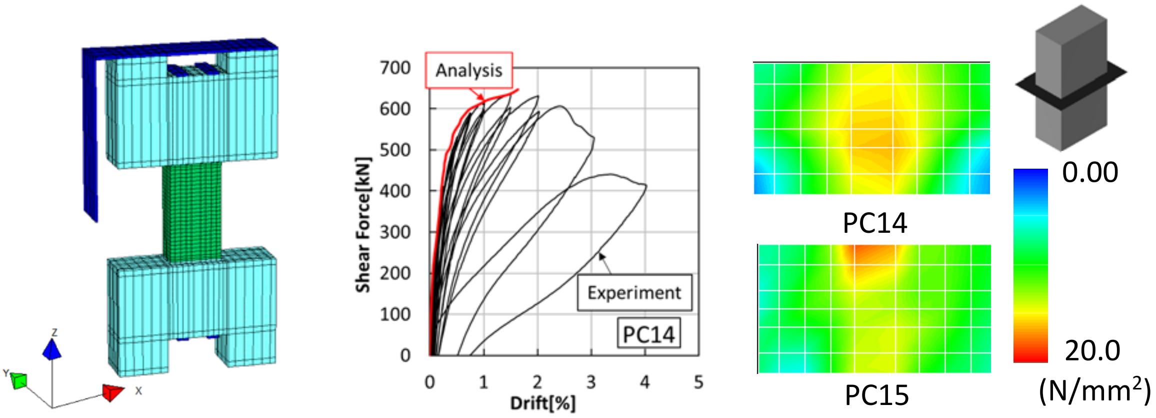

(a) Analytical model (b) Calculated shear force - Drift relation (c) Minimum principal stress diagram

Figure 9: FEM analysis

7 CONCLUSIONS

This study aims to evaluate the shear performance of precast pre-stressed concrete beams using unbonded tendons through tests and analyses. The main findings are as follows:

1. The ultimate flexural strength and ultimate shear strength of unbonded PCaPC beams can be roughly evaluated using the formula proposed in the past, as shown in the references.
2. Shear crack resistance strength can be considered as the shear damage limit critical strength, and the flexural strength using $0.9\sigma_B$ triangular stress distribution of concrete can be considered as the flexural damage limit critical strength.
3. For the specimen with a shear span ratio of 1.0, the large number of shear reinforcements is effective on the shear force holding ability.
4. The strength at the large deformation was high and the damage was small for the specimen with tie bars compared with the one with the same shear reinforcement ratio without tie bars.
5. For the specimen with a shear span ratio of 1.5, the shear reinforcements are effective for restraining the concrete as lateral reinforcements at the end portion, and effects to the capacity holding ability.

REFERENCES

[1] Architectural Institute of Japan, Design Guidelines for Earthquake Resistant Reinforced Concrete of Buildings Based on Inelastic Displacement Concept, 1999.08 (in Japanese).
[2] Architectural Institute of Japan, Standard for Structural Design and Construction of Prestressed Concrete Structures, 1998.11 (in Japanese).
[3] ITOCHU Techno-Solutions Corporation: FINAL/V11 HELP, 2011.7 (in Japanese)
[4] Junichi Izumo, Hiroshi Shima, Hajime Okamura: Analytical Model for Reinforced Concrete Panel Elements Subjected to In-Plane Forces, Concrete Journal, No. 87.9-1, pp. 107-120, 1987.9 (in Japanese)
[5] Naganuma, K., Stress-Strain Relationship for Concrete under Tri-axial Compression, Journal of Structural and Construction Engineering (Transactions of AIJ), No. 474, pp. 163-170, 1995.8 (in Japanese)